Field Measurement and Numerical Simulation of Marine Environment around Mega-float Model in Tokyo Bay

Masataka FUJINO, Shigeru TABETA
Dept.of Environmental Studies, University of Tokyo
7-3-1 Hongo, Bunkyo-ku, Tokyo 113-8656, Japan
Yusaku KYOZUKA
Dept. Earth System Sci. and Tech., Kyushu University
6-1 Kasugakoen, Kasuga, Fukuoka 816-8560 , Japan

1 INTRODUCTION

For the purpose of realizing the ocean space utilization, construction of very large floating structures (VLFS) is now being considered in the various fields concerned. Recently in Japan, in order to promote research and development of VLFS and put them to practical use, Technological Research Association of Mega-float (TRAM) was organized in 1995 by the united effort of both Japanese industries of shipbuilding and steel making. TRAM constructed large floating structure models for field experiments and moored them off Oppama of Tokyo Bay shown in Figure 1. In the first experiment called Phase-1, which was carried out from 1995 to 1997, a floating structure model with horizontal scales of 300 meters by 60 meters was constructed for the purpose of research and development of elemental technologies to realize VLFS[1]. After then, the second experiment called Phase-2 started from 1998, which is planned to continue for three years[2]. In Phase-2 experiment, a larger floating structure model, whose length is 1000 meters and the maximum width is 120 meters, was constructed in order to examine the feasibility of VLFS for the utility as an airport. The locations of Phase-1 and Phase-2 models are shown in Figure 1.

It is expected that the impact of VLFS on the natural environment is insignificant. However, before the Mega-float projects started, there was little actual data proving that VLFS has less adverse effect on the surrounding environment. Therefore, it was an urgent matter to examine the extent of VLFS 's influence on marine environment. There are two main approaches to examine the environmental impact by VLFS. One of them is the direct monitoring of marine environment around such structures. The authors carried out continuous observation of physical environment such as water temperature and salinity below and around VLFS model in Phase-1 experiment of Mega-float project[3]. The other effective approach is numerical simulations. The authors also developed a numerical model to predict currents, temperature, salinity, and density field in estuaries under the influences of VLFS[4]. In this paper, some results of the field measurement and the numerical simulation carried out by the authors are reported.

2 FIELD MEASUREMENT FOR PHASE-1 MODEL

2.1 Measurement site and instruments

The Mega-float model for Phase-1 experiment had been moored off Oppama in Tokyo Bay from July 1996 till December 1998. The mooring site is at a distance of about 250m apart from a fitting out basin of the Oppama Shipyard of Sumitomo Heavy Industries (see Figure 2). The water depth of the mooring site ranges from 5m to 8m, and there exist two breakwaters in the vicinity of the model. One of them is located about 30m east of the model, and the other, the southeastward breakwater, ranges from northwest to southeast. The model is tightly fixed to four dolphins, of which three dolphins lie in the east side of the model and the remaining one does in the south side. However, the vertical displacement of the model is not restricted.

Two sets of thermometers are set at two different positions on the Mega-float model in order to clarify to what extent the sea-surface covering effect of the model affects the vertical distribution of water temperature around the model. Each set of thermometers consists of eleven sensors of water temperature, which are distributed along a single line at 0.5m or 1.0m spaces between two adjacent sensors (hereafter called "thermistorchain"). Ballast chains of 5kg were attached to the bottom end of each thermistorchain so that they could not be moved by current. One of these two thermistorchains is fixed to the vertical wall inside a manhole at the center of the Mega-float model (Station A in Figure 2), and the other one is set at the northwest corner of the model (Station B in Figure 2). Since these two thermistorchains are fixed to the floating structure, the vertical location of ther-

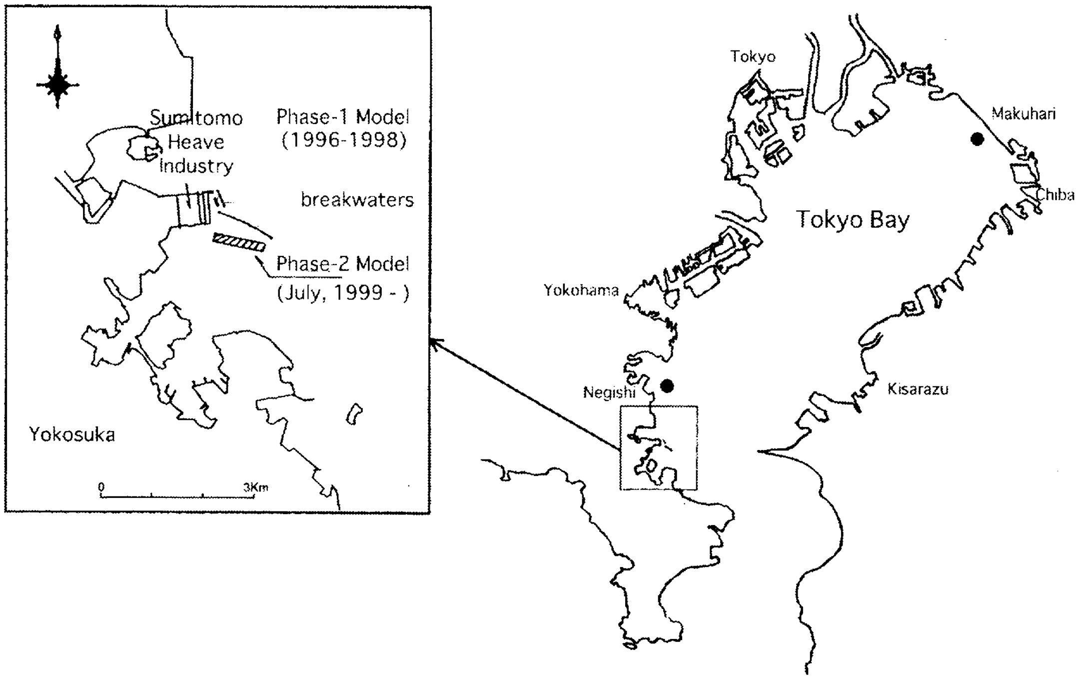

Figure 1: Mooring site of Mega-float Model in Tokyo Bay

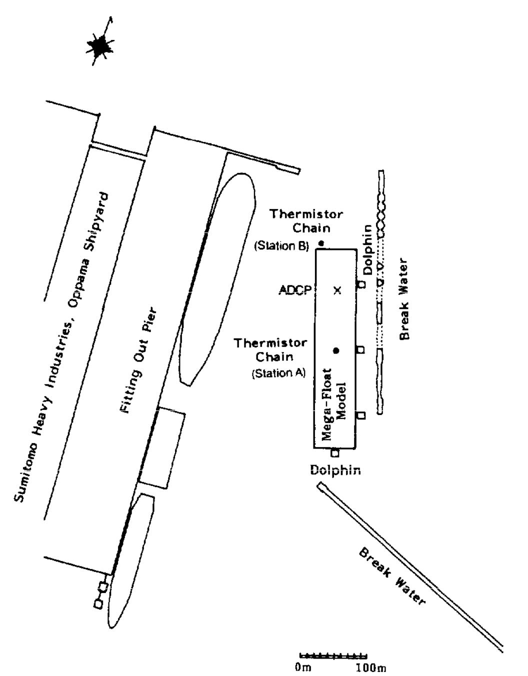

Figure 2: Mooring site in the vicinity of Mega-float Phase-1 Model

mometer keeps its constant depth under the water surface, regardless of change of the surrounding sea level. The clearances between the lowest thermometers and sea-bed were determined so that the lowest thermometers may not touch sea-bed even under the low water level. To the thermistorchain located at the northwest corner (Station B), two salinometers are tied at two vertical locations along the thermistorchain as shown in Figure 3. Table 2 shows specifications of sensors used for temperature and salinity measurements. The measured temperature and salinity are stored continuously in DSU (Data Store Unit) at 10 minute interval. The measurement of water temperature and salinity was started on 9th of August, 1996, and was continued till December 1998.

2.2 Results and discussion

Figures 4 and 5 show the time series of 24 hours' moving average of water temperature from August 1996 to July 1997 around the Mega-float model. In the figure, temperature of three vertical points at each station are shown as representatives. In summer season with high atmospheric temperature and large solar radiation, there exist vertical gradient of water temperature, where the water temperature near the surface is higher than those near the bottom.

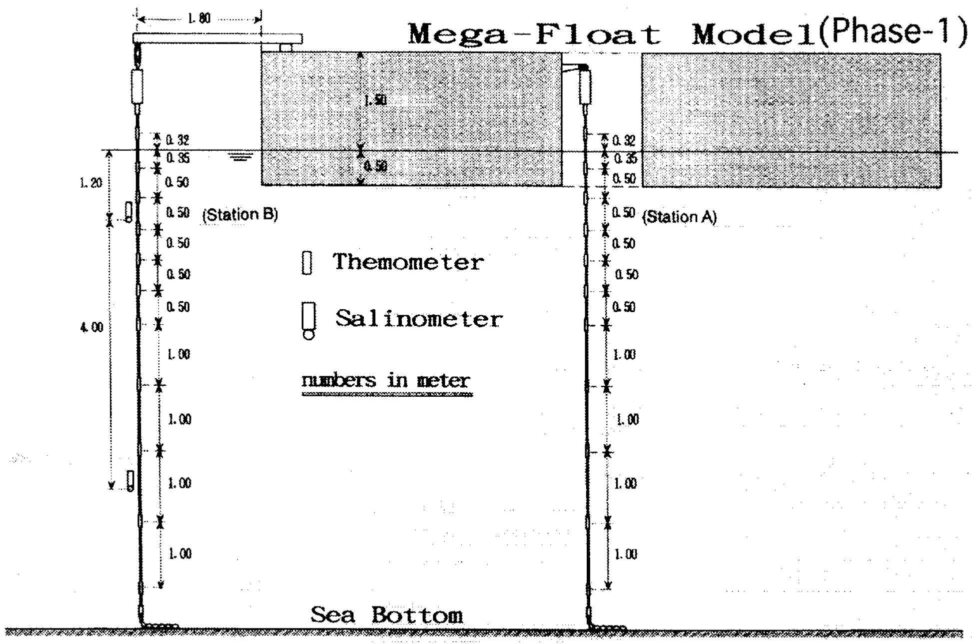

Figure 3: Setup of Water Temperature and Salinity Measurement

Table 1: Specifications of Sensors Used for Temperature and SalinityMeasurement

Sensors	Thermometer	Salinometer
Measuring range	-0.34°C ~ 32.17°C	Temperature: -5°C ~0°C Conductivity: 0~60mmho/cm
Measuring resolution	0.1% of the range	Temperature: 0.01°C Conductivity: 0.01mmho/cm
Accuracy of measurement	±0.05°C	Temperature ±0.05°C Conductivity: ±0.1mmho/cm

On the other hand, in winter season with low atmospheric temperature and small solar radiation, the vertical difference of water temperature was scarcely seen. Figure 6 shows the time series of 24 hours' moving average of salinity from January to June 1997 at Station B. It is found that both of vertical difference and temporal variation of salinity are larger in summer than winter.

The primary purpose of the present measurement is to clarify the influence of sea-surface covering effect of a large floating structure. For this purpose, one of the measurement stations (Station A) is located at the center of the Mega-float model where the sea surface is covered by the floating body, and the other station (Station B) is located at open sea. However, it can be said that there was little difference of water temperature between the two measurement stations from Figures 4 and 5. In order to investigate the influence of the floating structure in detail, a histogram of temperature difference between Station A and Station B is shown in Figure 7. It is found that the difference of temperature is under 0.3 °C for 97.4% of the total data, and it is under 0.5 °C for 99.4% of the total data. It is because tidal current and corresponding drift of water body are large in comparison with the horizontal scale of the floating structure in the present case. The horizontal drift of water body by tidal current can be estimated to be several kilometers when the maximum current speed is several tens centimeters per second. Therefore, it is supposed that there is little water which stays below the floating structure during a tidal period.

Figure 8 shows the cross correlation coefficient of water temperature variation at Station A and B. The correlation between the two stations is very strong and the correlation coefficient becomes largest when the phase difference is about 10 minute. Figure 9 shows the scattering diagram of current velocity below the floating structure, which is measured with ADCP provided by TRAM. It shows that the current

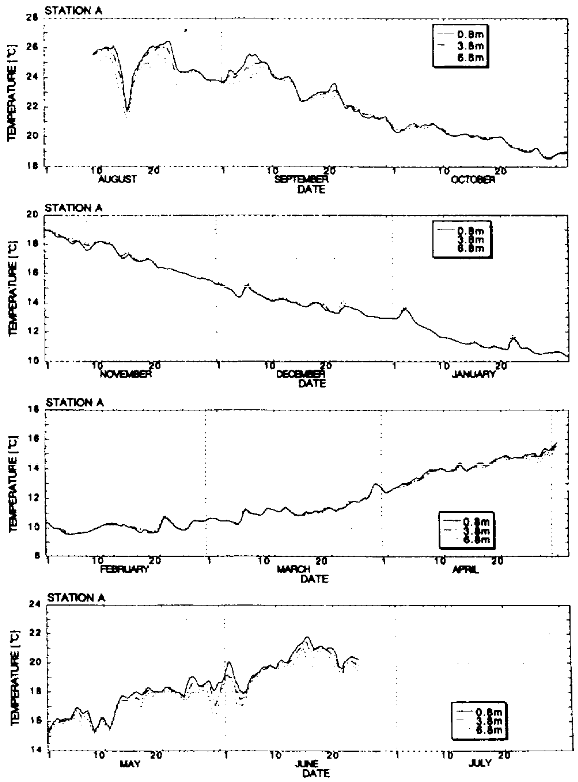

Figure 4: Time series of water temperature observed at Station A

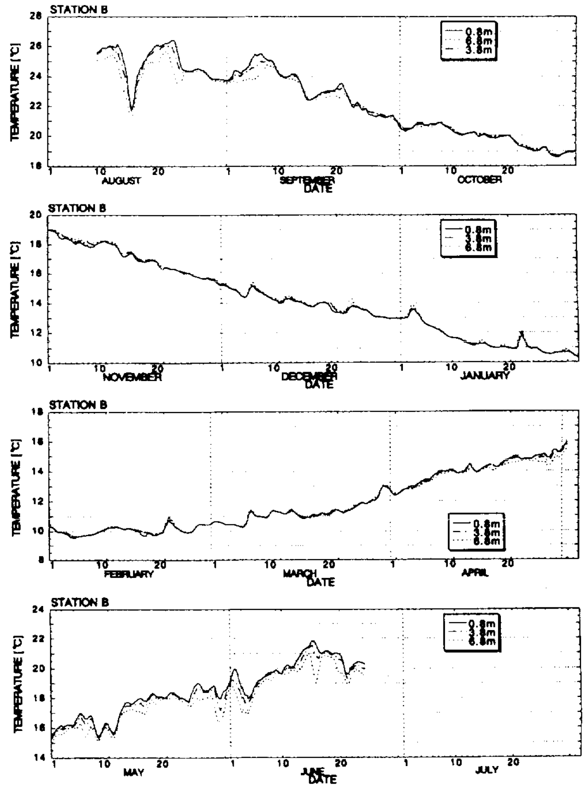

Figure 5: Time series of water temperature observed at Station B

velocity under the floating structure flows toward southwestward direction with average velocity of 0.08 m/sec. From these facts, it is indicated that the water temperature change under the floating structures strongly affected by the that at north part of the Mega-float model.

3 NUMERICAL SIMULATION OF PHYSICAL ENVIRONMENT

3.1 Discription of numerical model and conditions for calculation

Another indispensable method for the environmental impact assessment of VLFS is numerical simulations. Although some numerical simulations had been carried out to examine the environmental impact of VLFS, they intended to reproduce the seasonally averaged filed under the constant boundary conditions. However, numerical simulations with temporary varying boundary conditions are necessary in order to verify the applicability of a numerical model for dynamically changing real phenomena. The continuous observation data around the Mega-float model is very useful for the verification of the results of numerical simulations. In the present study, the time series of observed field data such as solar radiation, wind, and so on were used as the boundary conditions of the numerical simulation in order to compare the numerical results with field data directly.

A multilevel model which have been developed for the calculations of estuary circulation was employed for the numerical simulation of marine environment around Mega-float model. The basic equations for current are Reynolds' equation, in which hydrostatic approximation is used in vertical motion, and the equation of continuity:

$$\frac{Du}{Dt} = -\frac{1}{\rho_0}\frac{\partial p}{\partial x} + fv + A_M\left(\frac{\partial^2 u}{\partial x^2} + \frac{\partial^2 u}{\partial y^2}\right) + \frac{\partial}{\partial z}\left(K_M\frac{\partial u}{\partial z}\right) \tag{1}$$

$$\frac{Dv}{Dt} = -\frac{1}{\rho_0}\frac{\partial p}{\partial y} - fu + A_M\left(\frac{\partial^2 v}{\partial x^2} + \frac{\partial^2 v}{\partial y^2}\right) + \frac{\partial}{\partial z}\left(K_M\frac{\partial v}{\partial z}\right) \tag{2}$$

$$0 = -\frac{1}{\rho}\frac{\partial p}{\partial z} - g \tag{3}$$

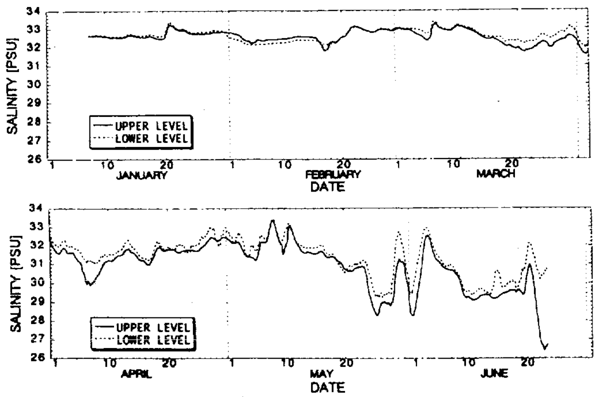

Figure 6: Time series of salinity observed at Station B

$$\frac{\partial u}{\partial x}+\frac{\partial v}{\partial y}+\frac{\partial w}{\partial z}=0 \qquad (4)$$

In these equations, f is Coriolis parameter; t is time; ρ is the density of sea water; ρ_0 is a constant reference density; p is the pressure; g is the acceleration of gravity; A_M is the coefficient of horizontal eddy viscosity; and K_M is the coefficient of vertical eddy viscosity. Water temperature T and salinity S are also calculated by the following equations:

$$\frac{DT}{Dt}=A_C(\frac{\partial^2 T}{\partial x^2}+\frac{\partial^2 T}{\partial y^2})+\frac{\partial}{\partial z}(K_C\frac{\partial T}{\partial z}) \qquad (5)$$

$$\frac{DS}{Dt}=A_C(\frac{\partial^2 S}{\partial x^2}+\frac{\partial^2 S}{\partial y^2})+\frac{\partial}{\partial z}(K_C\frac{\partial S}{\partial z})-\frac{RS}{V_R} \qquad (6)$$

where A_C is the coefficient of horizontal eddy diffusivity, K_C is the coefficient of vertical eddy diffusivity, and R is river discharge per unit time, which flows into the volume V_R which is taken to be the volume of the top level mesh where the river mouth is located. The density of sea water is assumed to be a function of temperature and salinity, and it is evaluated by the following formula:

$$\begin{aligned}\rho = 1028.14 - 0.0735T - 0.00469T^2 \\ +(0.802-0.002T)(S-35.0)\end{aligned} \qquad (7)$$

At the sea bottom and at the closed boundary, no-slip condition is used and the heat and salinity fluxes through the boundaries are assumed to be zero. At the open boundary, the sea level and the salinity of outer sea are given, and gradients of current velocity and water temperature are assumed to be zero. At the surface of the sea, the wind stress $\boldsymbol{\tau}$, upward heat flux per unit time and per unit area Q_T, and salinity flux Q_S, are given as follows:

$$\boldsymbol{\tau} \;=\; \rho_a C_d \boldsymbol{W}|\boldsymbol{W}| \qquad (8)$$

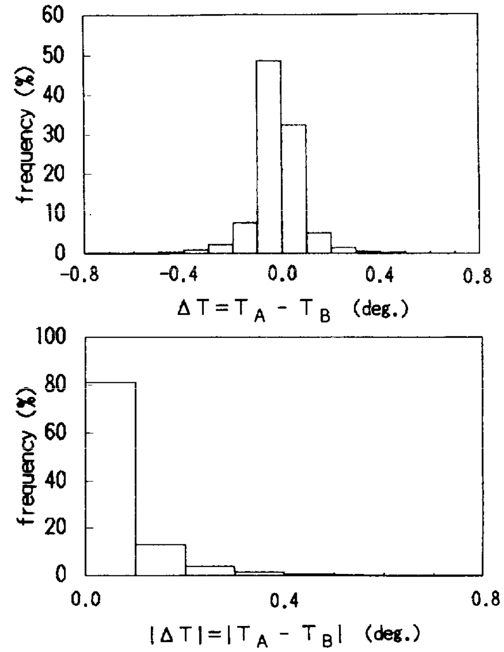

Figure 7: Histogram of temperature difference between Station A (T_A) and Station B (T_B) (August 1996 ~ June 1997:total number of data N=45441)

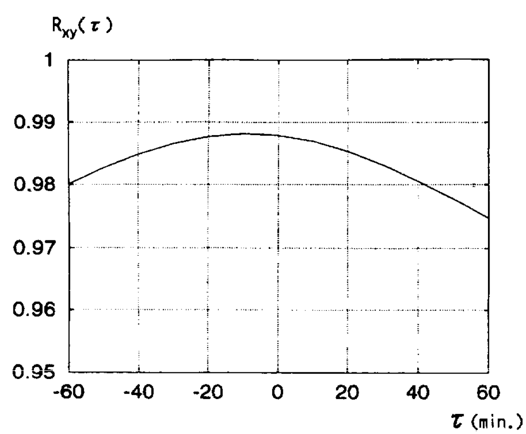

Figure 8: Cross correlation coefficient of water temperature at Station A and B (August to December 1996)

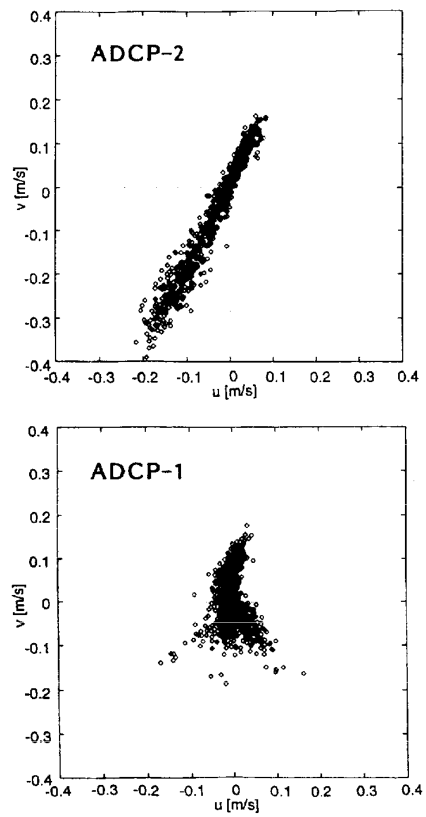

Figure 9: Scattering diagram of current velocity under the Mega-float model observed by ADCP in October 1996

$$Q_T = -Q_s + Q_b + Q_e + Q_c \quad (9)$$
$$Q_S = S(P_r - E_{vap}) \quad (10)$$

where ρ_a is the density of the atmosphere; C_d is the drag coefficient at the sea surface; $\boldsymbol{W}$ is wind vector; P_r is precipitation rate; and E_{vap} is evaporation rate. The heat flux through the sea surface Q_T is assumed to be composed of four components: global solar radiation Q_s, effective back radiation Q_b, latent heat transport by evaporation Q_e, and sensible heat transport by convection or conduction Q_c. Q_s, Q_b, Q_e, Q_c, and E_{vap} are calculated by using atmospheric data, such as wind speed, atmospheric temperature, vapor pressure or relative humidity, cloud amount, and precipitation.

When the sea water stratifies, the density gradient suppresses the vertical turbulent transportation of momentum, heat, and salinity. In order to consider this effect, the following formulae are used for evaluating vertical eddy viscosity and diffusivity co-

Table 2: Parameters used in the numerical simulation

Symbol	Value
$g(m/s2)$	9.807
$f(rad/s)$	$8.42 \times 10 - 5$
$\rho_0(kg/m3)$	1020.0
$A_M(m2/s)$	95.1
$K_{M0}(m2/s)$	0.0001
$A_C(m2/s)$	19.0
γ	0.0026
C_d	0.0015
$\rho_a(kg/m3)$	1.147
$Cp(J/kg/K)$	3.930×10^3

efficients.

$$\frac{K_M}{K_{M0}} = (1 + 5.2R_i)^{-1} \quad (11)$$
$$\frac{K_C}{K_{M0}} = (1 + \frac{10}{3}R_i)^{-1.5} \quad (12)$$

where K_{M0} is the vertical eddy viscosity coefficient under homogeneous condition, and R_i is the Richardson Number defined as the following formula.

$$R_i = -\frac{g \cdot \partial\rho/\partial z}{\rho(\partial U/\partial z)^2} \quad (13)$$

By using the numerical model described above, the physical environment such as current, water temperature and salinity in Tokyo Bay were calculated for the summer of 1996. The main paremeters used in the simulation are shown in Table 2.

3.2 Results and discussion

Figure 10 shows time series of water temperature, salinity observed off Oppama from 8 August to 8 September in 1996. In the figure, water temperature off Negishi and off Makuhari, which were measured and provided by other institutes, are also shown (see Figure 1 for the locations). Figure 11 shows time series of the amount of solar radiation, atmospheric temperature and wind velocity observed off Oppama, and sea level at Yokosuka during the same period.

For the water temperature at upper layer, the diurnal change is much larger than the semidiurnal change. It is because the sea water near the surface is strongly affected by solar radiation. On the other hand, semidiurnal mode is as large as diurnal one for the water temperature at lower layer. The amplitude of semidiurnal mode changes for the period of about half a month, which is corresponding to spring-neap tidal cycle. The vertical gradient of water temperature disappears when solar radiation is relatively small. However, the stratification remains

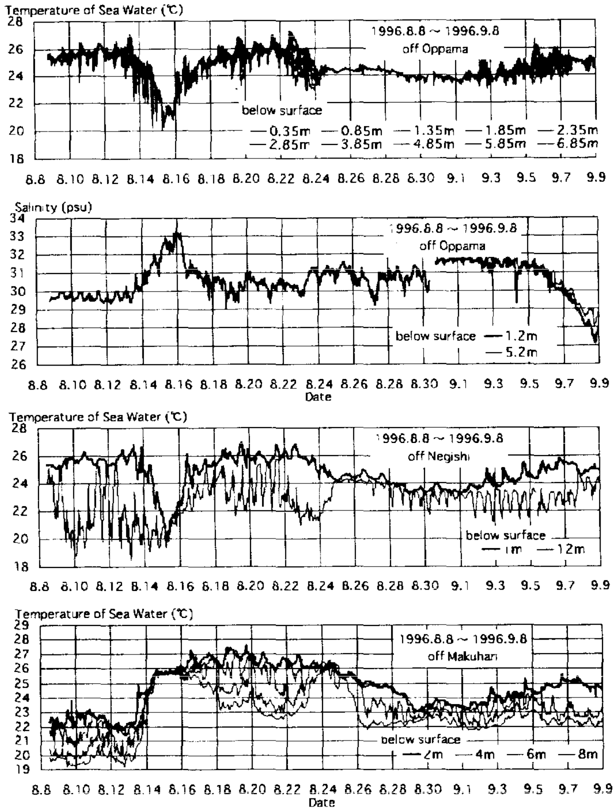

Figure 10: Time histories of water temperature, salinity observed off Oppama, water temperature observed off Negishi, and water temperature observed off Makuhari (8 August - 8 September, 1996)

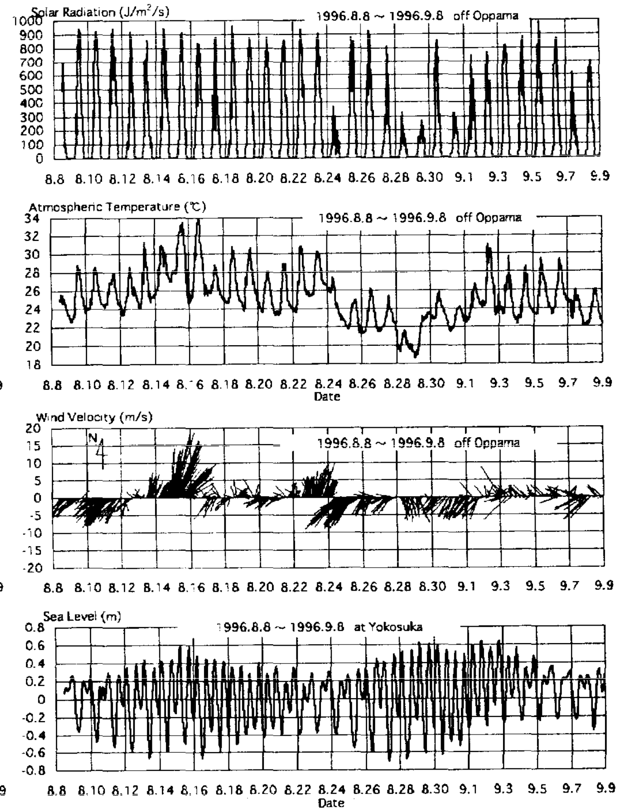

Figure 11: Time histories of the amount of solar radiation, atmospheric temperature and wind velocity observed off Oppama, and sea level at Yokosuka (8 August - 8 September, 1996)

almost always during the period of neap tide, when tidal currents are relatively small. At western coast of the bay, Oppama and Negishi, there were sudden drop of water temperature at about 15 August. At the same time, salinity increased rapidly. This phenomenon was due to coastal upwelling caused by strong southwesterly wind.

Figure 12 shows corresponding numerical results of water temperature and salinity off Oppama, off Negishi, and off Makuhari. The temporal and spatial difference of amplitude of diurnal and semidiurnal change of water temperature and salinity shows same tendency as the field data. The temperature change by coastal upwelling observed at about 15 August is also described successfully. However, the salinity restoration after the upwelling cannot be reproduced well. One of the reason is supposed that the accuracy of river discharge data was not enough.

It can be said that the numerical model used in the present study can predict the dynamic change of physical environment in estuaries fairly well.

4 RESEARCH PLAN FOR PHASE-2 MODEL

In Phase-1 experiment the authors mainly investigated the oceanophysical environment such as water temperature and salinity around the Mega-float model. It was found that the influence of Phase-1 model on the surrounding physical environment is almost negligible. One of the reason is supposed that the floating structure model of Phase-1 experiment was not so large. Therefore, the authors decided to continue the monitoring of physical environment for Phase-2 model, which has much larger horizontal scale than Phase-1 model. The measurement started July 1999, and are also carried out at two different stations below and around the Mega-float model.

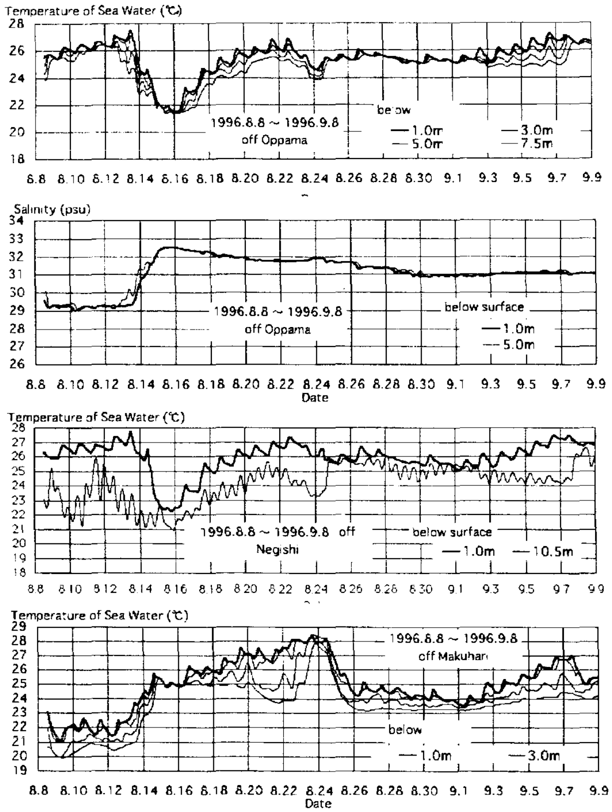

Figure 12: Predicted water temperature, salinity off Oppamam water tempereture off Negishi, and waer temperature off Makuhari

When considering the influences of Mega-float on marine ecosystem or material circulation, chemical or biological environment are essential. In the field observation in Phase-2 experiment, continuous monitoring of dissolve oxygen and Chlorophyll-a, which are important indexes for biological environment, are measured additionally. The monitoring of nutrient is also planned in order to understand the mechanism of ecosystem at the sea area where Mega-float model is located.

Corresponding to the field measurement, the numerical simulations by a model including ecosystem will be carried out, in order to make validation of the model and to understand the variation process of ecosystem.

5 CONCLUDING REMARKS

The university researchers including authors have carried out the investigation of marine environment around large artificial structures under the cooperation of TRAM. By the continuous monitoring of the marine environment around Mega-float model, precious filed data was obtained not only for the investigation of the influences of VLFS on physical environment but also the grasp of the actual dynamic process of the coastal phenomena. It is also found that the present numerical model can be an effective tool to predict the dynamic oceanophysical process in the estuary. The research about marine environment around Mega-float is still continued, and more detailed information about the phenomena in the measurement area are expected to be obtained.

The authors wish to express sincere thanks to the TRAM, which kindly cooperated in the present study.

REFERENCES

1) Technological Research Association of Mega-float: Report on the results of studies about very large floating structures (Part 1) (in Japanese), Bulletin of Soc. Nav. Archit. Japan, Vol.838 (1999)

2) E.Isobe: On the research in Mega-float Phase-2 (in Japanese), Bulletin of Soc. Nav. Archit. Japan, Vol.834 (1998)

3) M.Fujino, Y.Kyozuka, S.Tabeta, Y.Okawa, et al. : Measurement of Oceanophysical Environment around Mega-float Model Moored in Tokyo Bay (in Japanese), Jour. Soc. Nav. Archit. Japan, Vol.182 (1997)

4) M.Fujino, Y.Kyozuka, S.Tabeta, D.kitazawa, Y.Knaai: A study on real time simulation of oceanophysical environment in Tokyo Bay (in Japanese), Jour. Soc. Nav. Archit. Japan, Vol.186 (1999)